AD-A121 042 ON THE NUMBER OF DEGREES OF FREEDOM USED BY AN ADAPTIVE 1/1
ANTENNA ARRAY IN A NON-NARROWBAND NOISE ENVIRONMENT(U)
NAVAL RESEARCH LAB WASHINGTON DC K R GERLACH 30 SEP 82
UNCLASSIFIED NRL-8632 F/G 9/5 NL

END

FILMED

DTIC

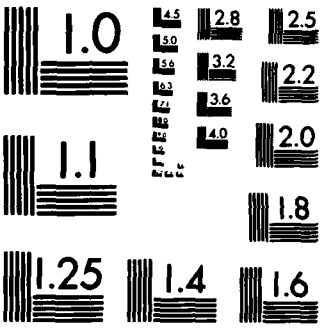

NRL Report 8632

On the Number of Degrees of Freedom Used by an Adaptive Antenna Array in a Non-Narrowband Noise Environment

KARL GERLACH

Airborne Radar Branch
Radar Division

September 30, 1982

NAVAL RESEARCH LABORATORY
Washington, D.C.

SECURITY CLASSIFICATION OF THIS PAGE (When Data Entered)

REPORT DOCUMENTATION PAGE		READ INSTRUCTIONS BEFORE COMPLETING FORM
1. REPORT NUMBER NRL Report 8632	2. GOVT ACCESSION NO. AD-A121042	3. RECIPIENT'S CATALOG NUMBER
4. TITLE (and Subtitle) ON THE NUMBER OF DEGREES OF FREEDOM USED BY AN ADAPTIVE ARRAY IN A NON-NARROWBAND NOISE ENVIRONMENT		5. TYPE OF REPORT & PERIOD COVERED Interim report on a continuing NRL problem 6. PERFORMING ORG. REPORT NUMBER
7. AUTHOR(s) Karl R. Gerlach		8. CONTRACT OR GRANT NUMBER(s)
9. PERFORMING ORGANIZATION NAME AND ADDRESS Naval Research Laboratory Washington, DC 20375		10. PROGRAM ELEMENT, PROJECT, TASK AREA & WORK UNIT NUMBERS PE62712N-XF12-141-370 53-0750-A-2
11. CONTROLLING OFFICE NAME AND ADDRESS Naval Electronic Systems Command Washington, DC 20360		12. REPORT DATE September 30, 1982 13. NUMBER OF PAGES 17
14. MONITORING AGENCY NAME & ADDRESS(if different from Controlling Office)		15. SECURITY CLASS. (of this report) UNCLASSIFIED 15a. DECLASSIFICATION/DOWNGRADING SCHEDULE

16. DISTRIBUTION STATEMENT (of this Report)

Approved for public release; distribution unlimited.

17. DISTRIBUTION STATEMENT (of the abstract entered in Block 20, if different from Report)

18. SUPPLEMENTARY NOTES

19. KEY WORDS (Continue on reverse side if necessary and identify by block number)

Antenna
Array
Adaptive

20. ABSTRACT (Continue on reverse side if necessary and identify by block number)

The relative measures of the eigenvalues of the noise covariance matrix of an adaptive array which is subjected to a non-narrowband jamming source are investigated. These measures are important because they determine the convergence rate and the upper limit of the output signal-to-noise ratio of the adaptive array. It is found that the adaptive array's performance as measured by the output signal-to-noise ratio degrades in quantum jumps as the input noise bandwidth increases. A methodology is developed whereby given the number of elements of the array, the array spacing, the array element antenna pattern, the power, and direction of arrival of an external jammer, these discrete bandwidths of the jammer that limit the output signal-to-noise ratio can be calculated.

DD FORM 1 JAN 73 1473 EDITION OF 1 NOV 65 IS OBSOLETE
S/N 0102-014-6601

SECURITY CLASSIFICATION OF THIS PAGE (When Data Entered)

CONTENTS

ON THE NUMBER OF DEGREES OF FREEDOM USED BY AN ADAPTIVE ANTENNA ARRAY IN A NON-NARROWBAND NOISE ENVIRONMENT

INTRODUCTION

It has been known for some time that the eigenvalues of the input noise covariance matrix associated with the optimal weighting of a linear adaptive array directly affect the performance of the adaptive array [1-5]. The optimal weights, W, are given by

$$W = \mu M^{-1} S, \tag{1}$$

where M is the $n \times n$ covariance matrix of the input noise that is received on each of the antenna elements, n is the number of antenna elements, S is the steering vector of the array, W represents the set of optimal weights in vector form, and μ is an arbitrary nonzero scalar. The set of weights given by Eq. (1) is optimum in the sense that the steady-state signal-to-noise ratio is maximized. Figure 1 illustrates the weighting of the array inputs. We assume that the input noises are stationary processes so that M is a constant. We now give some examples of how the eigenvalues affect the performance-measures of an adaptive array.

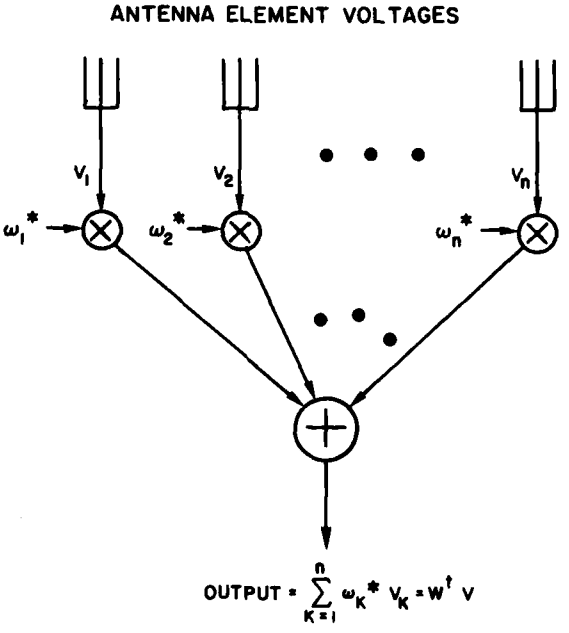

Fig. 1 — Adaptive array

Manuscript submitted June 24, 1982.

For a control-loop implementation of Eq. (1), the eigenvalues of M are related to the time constants of adaptation and the control-loop noise [3]. If λ_k, $k = 1, \ldots, n$ are the eigenvalues of M, then the time constants of adaptation, τ_k, are given by

$$\tau_k = \frac{1}{\lambda_k}. \tag{2}$$

Hence the time constants are inversely proportional to the eigenvalues. In addition, it can be shown that the control-loop noise power is approximately proportional to the sum of the eigenvalues if the input noise is approximately wideband [3].

For any implementation, if the optimal weights are employed to form the antenna pattern, then it can be shown that the steady state signal-to-noise power ratio, (S/N), is given by

$$\left(\frac{S}{N}\right) = S^t M^{-1} S \tag{3}$$

where t denotes conjugate transpose.

Since M is hermitian, it is possible to write M in the form

$$M = \Phi^t \Lambda \Phi \tag{4}$$

where Φ is a nonsingular $n \times n$ unitary matrix and Λ is a diagonal matrix of the positive real eigenvalues of M ($\Lambda = (\lambda_k)$), $k = 1, \ldots, n$. Using Eq. (4) and Eq. (3), we can show that

$$\left(\frac{S}{N}\right) = \sum_{k=1}^{n} \frac{1}{\lambda_k} ||\Phi_k S||^2 \tag{5}$$

where Φ_k is the kth row of the matrix Φ (it is also an eigenvector of M) and $||\cdot||$ signifies the magnitude of the complex argument. Thus, we see from Eq. (5) that increasing the values of the eigenvalues has a tendency to decrease the output signal-to-noise ratio. Also, the smaller eigenvalues limit the maximum value of (S/N).

In this report, we consider the distribution of the eigenvalues for the case when the noise environment consists of internal noises and a single, external, spatially distinct, non-narrowband noise source (jammer). The distribution of the eigenvalues will change as we change the bandwidth of the jammer. We show that as the bandwidth of the jammer increases, then the smaller eigenvalues of M increase. More importantly, we show that only one of the smaller eigenvalues increases significantly for small percentage bandwidths. Hence, from Eq. (5), we see that the output signal-to-noise ratio will suffer accordingly. In addition we also develop a methodology whereby this increase in the smaller eigenvalues can be calculated as a function of the percentage bandwidth of the jammer, the number of array elements, the angle of arrival of the jammer, the power of the jammer, and the array element antenna pattern. It is important to note that the results presented in this report are *not* applicable to adaptive sidelobe cancellation schemes. We assume that *all* the antenna elements of an array can be adaptively controlled.

COVARIANCE MATRIX DEFINITION

If $V = (v_1, v_2, \ldots, v_n)^T$ denotes the input vector of the noise on each antenna element where T denotes transpose, then

$$M = E\{V V^t\}, \tag{6}$$

where $E\{\bullet\}$ denotes expectation. Let us write M as

$$M = \sigma_0^2 \mathrm{I} + M_J, \tag{7}$$

where σ_0^2 is the internal noise power, I is the $n \times n$ identity matrix, and M_J is the covariance matrix of the external noise sources. Define

$$\hat{M} = \frac{1}{\sigma_0^2} M = \mathrm{I} + \frac{1}{\sigma_0^2} M_J. \tag{8}$$

From Eq. (3), we can show that

$$\left(\frac{S}{N}\right) = \frac{1}{\sigma_0^2} S' \hat{M}^{-1} S. \tag{9}$$

If $\hat{\lambda}_k$, $k = 1, \ldots, n$ are the eigenvalues of $\hat{M}$, then

$$\lambda_k = \sigma_0^2 \hat{\lambda}_k \quad k = 1, \ldots, n. \tag{10}$$

Hence, if we find the distribution of $\hat{\lambda}_k$, $k = 1, \ldots, n$, we can easily find the distribution of λ_k, $k = 1, \ldots, n$ by using σ_0^2 as a scaling factor. In the following analysis we will consider the distribution of the eigenvalues of $\hat{M}$.

Let us also normalize M_J to σ_0^2, so that $\hat{M}_J = M_J/\sigma_0^2$ and

$$\hat{M} = \mathrm{I} + \hat{M}_J. \tag{11a}$$

We recognize that the eigenvalues of $\hat{M}_J$ are related to the eigenvalues of $\hat{M}$ by the expression

$$\hat{\lambda}_k = \hat{\lambda}_{J_k} + 1 \quad k = 1, \ldots, n. \tag{11b}$$

If there is only one external jammer and $\hat{M}_J = (\hat{m}_{ij})$, $i, j = 1, \ldots, n$, then it has been shown [6] that

$$\hat{m}_{ij} = P_J ||g_e(\theta)||^2 \rho_{ij}(\tau) \exp\left[I \frac{2\pi}{\lambda_0} (d_i - d_j) \sin\theta\right], \tag{12}$$

where θ is the angle off boresight of the jammer, $g_e(\theta)$ is the element gain function, d_i and d_j are the distances of the ith and jth elements from a reference point on the array, λ_0 is the wavelength of the carrier frequency, f_0, of the jammer, $I = \sqrt{-1}$, P_J is the input power of the jammer at any antenna element normalized to the internal noise power,

$$\rho_{ij}(\tau) = \frac{\sin(\pi B \tau_{ij})}{\pi B \tau_{ij}}, \tag{13}$$

and

$$\tau_{ij} = \frac{d_i - d_j}{c} \sin\theta. \tag{14}$$

In Eq. (13), B is the bandwidth of the input noise and in Eq. (14), c is the speed of light. Equation (13) assumes a rectangular bandpass for the jammer. If $B = 0$ then $\rho_{ij}(\tau) = 1$ and Eq. (12) reduces to

$$\hat{m}_{ij} = P_j ||g_e(\theta)||^2 \exp\left\{I \frac{2\pi}{\lambda_0} (d_i - d_j) \sin\theta\right\}. \tag{15}$$

Equation (15) corresponds to the narrowband approximation that has been used often to evaluate the performance of the adaptive array [1-5]. It can be shown that if the input noise is narrowband, then the eigenvalues of $\hat{M}$ are given by

$$\hat{\lambda}_1 = nP_J \, ||g_e(\theta)||^2 + 1, \tag{16}$$

and

$$\hat{\lambda}_k = 1 \qquad k = 2, \ldots, n. \tag{17}$$

Hence $n - 1$ of the eigenvalues are equal.

TYPICAL EIGENVALUES

In this section, we present an example of the computed eigenvalues of the covariance matrix given by Eq. (12). For all cases, we set the number of antenna elements n equal to 8 and fix $\theta = 45°$. We vary the percentage bandwidth of the jammer (defined as 100 B/f_0) from 0 to 14% in increments of 2% and consider two different normalized jammer powers: 10 dB and 20 dB. The eigenvalues for the various cases are presented in ascending order in Tables 1 and 2.

Table 1 — Eigenvalues *vs* Percent Bandwidth
($n = 8$, $\theta = 45°$, $P_J = 10$ dB)

Eigen-value	Percent Bandwidth							
	0	2	4	6	8	10	12	14
λ_8	1.0	1.0	1.0	1.0	1.0	1.0	1.0	1.0
λ_7	1.0	1.0	1.0	1.0	1.0	1.0	1.0	1.0
λ_6	1.0	1.0	1.0	1.0	1.0	1.0	1.0	1.0
λ_5	1.0	1.0	1.0	1.0	1.0	1.0	1.0	1.0
λ_4	1.0	1.0	1.0	1.0	1.0	1.0	1.0	1.0
λ_3	1.0	1.0	1.0	1.0	1.0	1.0	1.0	1.1
λ_2	1.0	1.1	1.5	2.2	3.1	4.3	5.7	7.2
λ_1	81.0	80.9	80.5	79.8	78.9	77.7	76.3	74.7

Table 2 — Eigenvalues *vs* Percent Bandwidth
($n = 8$, $\theta = 45°$, $P_J = 20$ dB)

Eigen-value	Percent Bandwidth							
	0	2	4	6	8	10	12	14
λ_8	1.0	1.0	1.0	1.0	1.0	1.0	1.0	1.0
λ_7	1.0	1.0	1.0	1.0	1.0	1.0	1.0	1.0
λ_6	1.0	1.0	1.0	1.0	1.0	1.0	1.0	1.0
λ_5	1.0	1.0	1.0	1.0	1.0	1.0	1.0	1.0
λ_4	1.0	1.0	1.0	1.0	1.0	1.0	1.0	1.0
λ_3	1.0	1.0	1.0	1.0	1.1	1.2	1.5	1.9
λ_2	1.0	2.4	6.5	13.2	22.5	34.0	47.6	62.9
λ_1	801.0	799.6	795.5	788.7	779.4	767.8	753.9	738.2

We note from Tables 1 and 2 that the sum of the eigenvalues is 88 in the first case and 808 in the second (the eigenvalues have been rounded off to the nearest first decimal place). An important property to note from these tables is that, as the percent bandwidth increases initially from 0%, only one of the smaller eigenvalues changes significantly (λ_2). Hence, it would appear that for a small percent bandwidth, only one eigenvalue is affected. This phenomenon has been reported in the literature by Gabriel [5] who showed empirically that a small percentage bandwidth jammer can require two degrees of freedom to be nulled effectively. It is quite fortunate that only one eigenvalue is significantly affected because we observe from Eq. (5) that this implies that only one term of the signal-to-noise ratio expression is involved.

As the jammer bandwidth increases, a number of the smaller eigenvalues will increase significantly. As the magnitudes of these eigenvalues increase, a corresponding larger number of degrees of freedom are needed to null the jammer. Hence the number of degrees of freedom needed to null a jammer is a function of the jammer bandwidth. Because the number of degrees of freedom is an integer, the jammer bandwidths where an extra degree of freedom is necessary to null a jammer will increase in discrete steps. We shall expand upon this topic later. Next, we demonstrate mathematically why this occurs and then we derive an approximate expression for the second largest eigenvalue.

ANALYSIS

Let us assume that the antenna elements are equispaced $d_{\lambda/2}$ half-wavelengths apart where $d_{\lambda/2}$ is not necessarily an integer. We set

$$\psi = \pi\, d_{\lambda/2} \sin\theta \tag{18}$$

$$\phi = \frac{\pi}{2}\, d_{\lambda/2}\, \frac{B}{f_0} \sin\theta \tag{19}$$

and

$$\bar{P}_J = P_J\, ||g_e(\theta)||^2. \tag{20}$$

The parameter ψ is the relative phase change between adjacent elements of the linear array due to the external jammer. The parameter ϕ is proportional to the jammer bandwidth ratio, B/f_0, element spacing, and the direction of arrival of the jammer. It is also proportional to the bandwidth aperture product. The parameter $\bar{P}_J$ is simply the output power due to the jammer from each of the antenna elements. The elements of the normalized noise covariance matrix now have the form

$$\hat{m}_{ij} = \bar{P}_J\, \frac{\sin(i-j)\phi}{(i-j)\phi}\, e^{I(i-j)\psi}. \tag{21}$$

We expand $\sin(i-j)\phi/(i-j)\phi$ into a Taylor series:

$$\frac{\sin(i-j)\phi}{(i-j)\phi} = 1 - \frac{1}{6}\phi^2(1-j)^2 + \frac{1}{120}\phi^4(i-j)^4 + O(\phi^6). \tag{22}$$

Hence,

$$\hat{m}_{ij} = \bar{P}_J e^{I(i-j)\psi} - \frac{1}{6}\bar{P}_J\phi^2(i-j)^2\, e^{I(i-j)\psi}$$

$$+ \frac{1}{120}\bar{P}_J\phi^2(i-j)^4\, e^{I(i-j)\psi} + O(\phi^6). \tag{23}$$

Using Eq. (23) and the definition

$$A_1(\psi) = (1,\, e^{I\psi},\, e^{2I\psi},\, \cdots,\, e^{(n-1)I\psi})^T \tag{24}$$

we can show that

$$\hat{M} = I + \bar{P}_J A_1 A_1^t + \frac{1}{6}\phi^2 \bar{P}_J \frac{d^2}{d\psi^2}(A_1 A_1^t)$$

$$+ \frac{1}{120}\phi^4 \bar{P}_J \frac{d^4}{d\psi^4}(A_1 A_1^t) + O(\phi^6). \tag{25}$$

It is straightforward to show that

$$\frac{d^2}{d\psi^2}(A_1 A_1^t) = \frac{d^2 A_1}{d\psi^2} A_1^t + 2\frac{dA_1}{d\psi}\frac{dA_1^t}{d\psi} + A_1 \frac{d^2 A_1^t}{d\psi^2}. \tag{26}$$

If we set

$$A_2 = (0, e^{I\psi}, 2e^{2I\psi}, \ldots, (n-1)\, e^{(n-1)I\psi})^T = -I\frac{dA_1}{d\psi}, \tag{27}$$

and

$$A_3 = (0, e^{I\psi}, 2^2 e^{2I\psi}, \ldots, (n-1)^2 e^{(n-1)I\psi})^T = -\frac{d^2 A_1}{d\psi^2}, \tag{28}$$

then it follows that

$$\hat{M} = I + \bar{P}_J A_1 A_1^t - \frac{1}{6}\phi^2 \bar{P}_J A_1 A_3^t$$
$$+ \frac{1}{3}\phi^2 \bar{P}_J A_2 A_2^t - \frac{1}{6}\phi^2 \hat{P}_J A_3 A_1^t$$
$$+ \frac{1}{120}\phi^4 \bar{P}_J \frac{d^4}{d\psi^4}(A_1 A_1^t) + O(\phi^6). \tag{29}$$

Furthermore, the above expression can be rewritten as

$$\hat{M} = I + \bar{P}_J\left(A_1 - \frac{\phi^2}{6} A_3\right)\left(A_1 - \frac{\phi^2}{6} A_3\right)^t$$
$$+ \frac{1}{3}\phi^2 \bar{P}_J A_2 A_2^t - \frac{1}{36}\phi^4 \bar{P}_J A_3 A_3^t$$
$$+ \frac{1}{120}\phi^4 \bar{P}_J \frac{d^4}{d\psi^4}(A_1 A_1^t) + O(\phi^6). \tag{30}$$

Let us define a column vector C such that

$$C = A_1 - \frac{\phi^2}{6} A_3. \tag{31}$$

Then $\hat{M}$ in Eq. (30) can be expressed as

$$\hat{M} = I + \hat{M}_J + O(\phi^4), \tag{32}$$

where

$$\hat{M}_J = \bar{P}_J C C^t + \frac{1}{3}\phi^2 \bar{P}_J A_2 A_2^t. \tag{33}$$

Notice from Eq. (33) that the matrix $\hat{M}_J$ has rank 2. Hence, $\hat{M}_J$ has exactly two nonzero eigenvalues. This implies that for small enough ϕ, $\hat{M}$ as expressed by Eq. (32) has two eigenvalues that will not be

equal to one. One of these eigenvalues will be large and the other will increase from the value 1 as ϕ increases. This phenomena is observed in Tables 1 and 2. We will refer to the two eigenvalues of $\hat{M}$ that are different from the value one as the dominant eigenvalues.

EIGENVALUE EVALUATION

In this section, we derive expressions for finding the dominant eigenvalues of $\hat{M}$ for small ϕ. Let $\hat{M} = I + \hat{M}_J$ where $\hat{M}_J$ is expressed by Eq. (33).

Let $\hat{\lambda}_{J_1}$ and $\hat{\lambda}_{J_2}$ be the nonzero eigenvalues of $\hat{M}_J$. (These eigenvalues of $\hat{M}_J$ are related to the dominant eigenvalues of $\hat{M}$ by Eq. (11b)).

It can be easily shown that for any $n \times n$ matrix Q with eigenvalues $\lambda_1, \lambda_2, \ldots, \lambda_n$,

$$\sum_{k=1}^{n} \lambda_1^n = \text{Trace } \{Q^n\}. \tag{34}$$

Hence, it follows that

$$\hat{\lambda}_{J_1} + \hat{\lambda}_{J_2} = \text{Trace}\{\hat{M}_J\}, \tag{35}$$

and

$$\hat{\lambda}_{J_1}^2 + \hat{\lambda}_{J_2}^2 = \text{Trace}\{\hat{M}_J^2\}. \tag{36}$$

Thus, we have two equations and two unknowns and we can solve for $\hat{\lambda}_{J_1}$ and $\hat{\lambda}_{J_2}$. We now evaluate the traces in Eqs. (35) and (36).

It is straightforward to show that

$$\text{Trace}\{\hat{M}_J\} = \bar{P}_J n. \tag{37}$$

Now we can calculate directly from Eqs. (31) and (33) that

$$\hat{M}_J^2 = \bar{P}_J^2 n A_1 A_1^t - \frac{1}{3}\bar{P}_J^2 n \phi^2 A_1 A_3^t + \frac{2}{3}\bar{P}_J^2 \phi^2 (A_1^t A_2) A_1 A_2^t$$
$$- \frac{1}{3}\bar{P}_J^2 \phi^2 (A_1^t A_e) A_1 A_1^5 + O(\phi^4). \tag{38}$$

From Eq. (38), we can evaluate the Trace$\{\hat{M}_J^2\}$. It is found that

$$\text{Trace}\{\hat{M}_J^2\} = \bar{P}_J^2 n^2 - \frac{1}{18}\bar{P}_J^2 \phi\, n^2(n^2 - 1) + O(\phi^4). \tag{39}$$

If we set $a_k = \text{Trace}\{\hat{M}_J^k\}$, $k = 1, 2$, it can be shown using Eqs. (35), (36), and the quadradic formula that

$$\hat{\lambda}_{J_k} = \frac{1}{2} a_1 \pm \frac{1}{2}\sqrt{2a_2 - a_1^2} \qquad k = 1, 2. \tag{40}$$

If we evaluate Eq. (40) for small ϕ, then it can be shown that

$$\hat{\lambda}_{J_1} = \bar{P}_J n - \frac{1}{36}\bar{P}_J \phi^2 n(n^2 - 1), \tag{41}$$

and

$$\hat{\lambda}_{J_2} = \frac{1}{36}\bar{P}_J \phi^2 n(n^2 - 1). \tag{42}$$

Hence, we see that one eigenvalue of $\hat{M}_J$ is large and decreasing as ϕ increases and the other eigenvalue is small (but nonzero) and increases as ϕ increases.

To measure at what jammer bandwidth the second eigenvalue becomes important to the nulling process, we define that point to be when $\hat{\lambda}_{J_2} = 1$. When $\hat{\lambda}_{J_2} = 1$, the covariance matrix $\hat{M}$ has an eigenvalue equal to two (see Eq. (11b)), and hence the signal-to-noise ratio (as expressed by Eq. (5)) will suffer moderate degradation. We define $(B/f_0)^{(2)}$ as the bandwidth-center frequency ratio where the second largest eigenvalue equals two. Note that this definition of a measure of adaptive processor performance is arbitrary. However, it can serve the same utility as the arbitrary definitions of bandwidth and antenna beamwidth where 3-dB attenuation points are used to define performance parameters.

The jammer bandwidth at which this occurs can be found using Eqs. (42), (19), and (20). It is found to be

$$\left(\frac{B}{f_0}\right)^{(2)} = \frac{12}{\pi} \frac{1}{d_{\lambda/2} \sin\theta \, (P_J ||g_e(\theta)||^2 \, n(n^2-1))^{1/2}}. \tag{43}$$

As a result, Eq. (43) implies that the bandwidth at which degradation will occur decreases as element separation, angle off-boresight, jammer power, element gain in the direction of the jammer, or the number of array elements increase.

RESULTS

Although we have derived an expression for $(B/f_0)^{(2)}$, Eq. (43), in the preceding section, it is extremely difficult to derive approximate expressions for $(B/f_0)^{(3)}$, $(B/f_0)^{(4)}$, ..., where $(B/f_0)^{(k)}$ is the bandwidth-to-center-frequency ratio and where the kth largest eigenvalue of $\hat{M}$ equals two. However, in this section, we develop a methodology where $(B/f_0)^{(k)}$, $k = 2, 3, 4$, can be found with the aid of graphs.

To this end, we first show that the eigenvalues of $\hat{M}_J$ are a function of ϕ, n, and $\bar{P}_J$ but not a function of ψ where ψ is the relative phase change between adjacent antenna elements due to the jammer. To prove this, we can show that if $\hat{M}_J = (c_{ij})$, then

$$\text{Trace}\,\{\hat{M}_J^L\} = \sum_{k_1=1}^{n} \sum_{k_2=1}^{n} \cdots \sum_{k_L=1}^{n} c_{k_1k_2} c_{k_2k_3} \cdots c_{k_{L-1}k_L} c_{k_Lk_1}. \tag{44}$$

Hence, since $\exp\{I(k_i - k_{i+1})\psi\}$ is a factor of $c_{k_ik_{i+1}}$, we see from Eq. (44) that all these factors cancel one another so that Trace $\{\hat{M}_J^L\}$ is independent of ψ. Now Eq. (34) implies that we can derive a nonlinear system of L equations with the L eigenvalues as unknowns. Thus, since no parameter of this system of equations is a function of ψ, the eigenvalues are not functions of ψ.

We also see from Eq. (12) that the eigenvalues of $\hat{M}_J$ are scaled by $\bar{P}_J$. Therefore we could plot $\lambda_J/\bar{P}_J$ *vs* ϕ and n, where λ_J is an eigenvalue of M_J.

However, for purposes of finding a graphical solution, we acquire λ_J in the following manner:

1. Use Figs. 2, 3, or 4 depending on whether the 2nd, 3rd, or 4th largest eigenvalue is desired.

2. Calculate ϕ as expressed by Eq. (19).

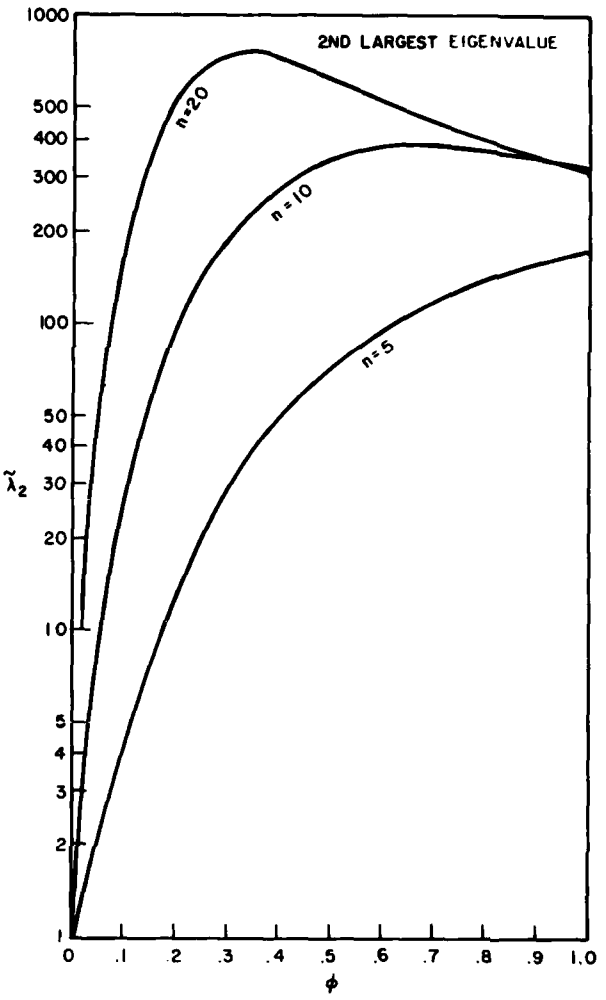

Fig. 2 — 2nd largest eigenvalue *vs* ϕ and n

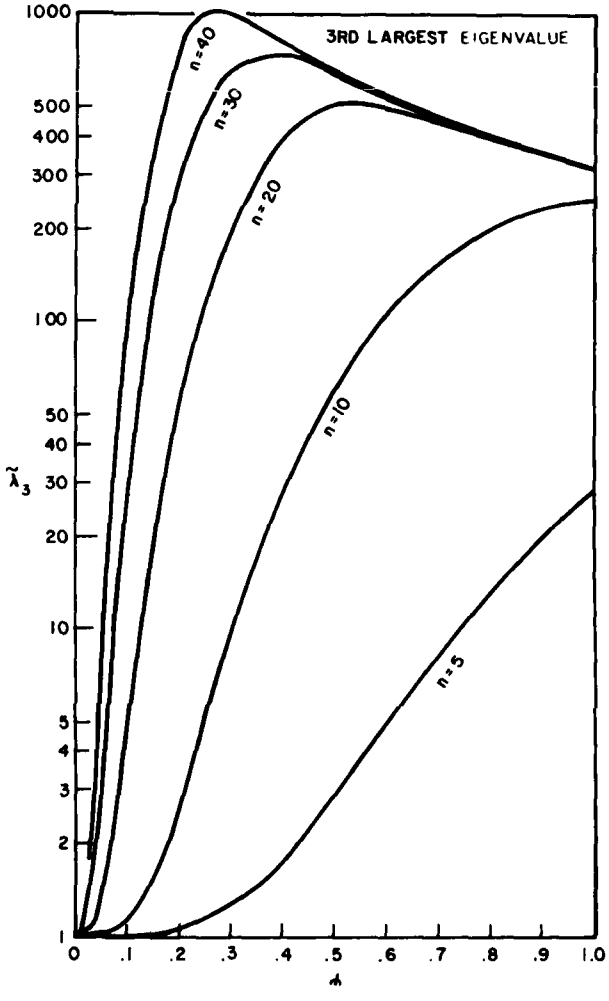

Fig. 3 — 3rd largest eigenvalue *vs* ϕ and n

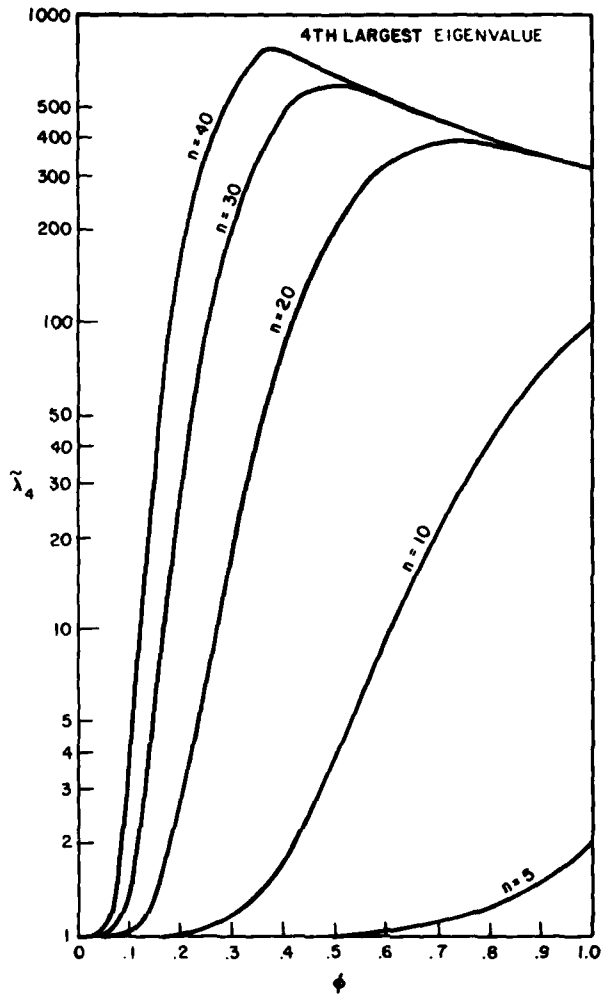

Fig. 4 — 4th largest eigenvalue *vs* ϕ and n

3. Find $\tilde{\lambda}_k$, $k = 2, 3, 4$ as a function of ϕ and n from graphs.

4. Find the eigenvalue scale factor, α_λ, as a function of $\bar{P}_J$ from Fig. 5.

5. The eigenvalue as a function of ϕ, N, and $\bar{P}_J$ is then

$$\lambda_k = \alpha_\lambda (\tilde{\lambda}_k - 1) + 1. \tag{45}$$

For example, if the jammer and array have the following characteristics:

(a) $n = 10$; (d) $||g_e(\theta)||^2 = 1$ (isotropic elements)

(b) $B/f_0 = 0.1$; (e) $d_{\lambda/2} = 1$ (half-wavelength spacing) (46)

(c) $\theta = 45°$; (f) $P_J = 30$ dB

then

$$n = 10\ ;\ \phi = 0.11;\ \bar{P}_J = 30 \text{ dB}.$$

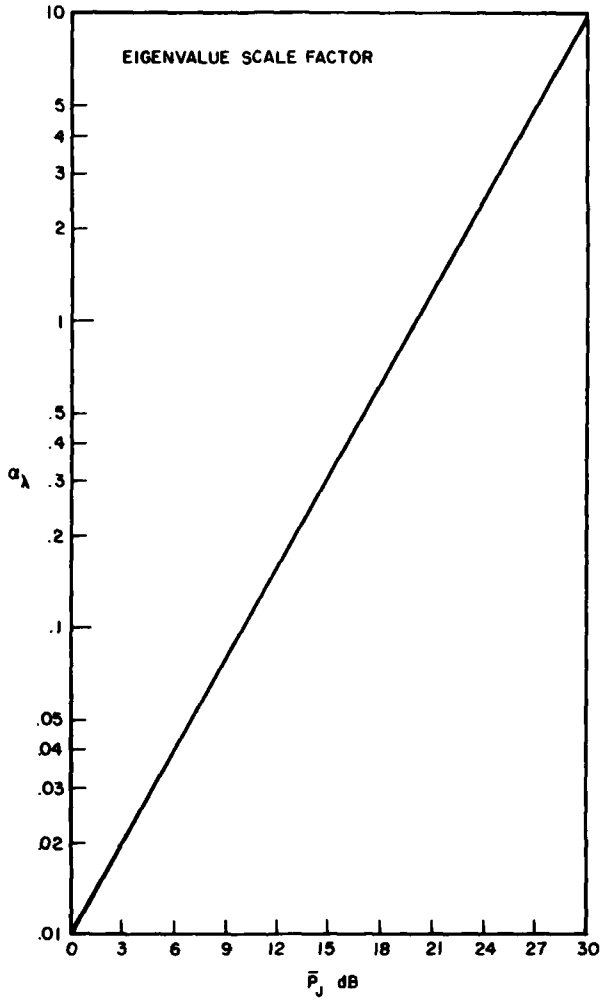

Fig. 5 — Eigenvalue scale vactor $\bar{P}_J$

Let us find the value of the third largest eigenvalue. We use Figs. 3 and 5 respectively to find that $\tilde{\lambda}_3 = 1.2$ and $\alpha_\lambda = 10.0$. Using Eq. (45) we find that the third largest eigenvalue is equal to three.

To find $(B/f_o)^{(k)}$ we use the following procedure: We plot as a function of n and $\bar{P}_j$, the value of ϕ that occurs when the 2nd, 3rd, or 4th eigenvalue equals two in Figs. 6, 7, and 8 respectively. We denote the values of ϕ that occur when the 2nd, 3rd, and 4th eigenvalues equal two as ϕ_2, ϕ_3, and ϕ_4 respectively. These curves can be obtained directly from using the curves in Figs. 2 through 5 by specifying the eigenvalue to be equal to two and working backwards to find ϕ_k, $k = 2, 3, 4$ as a function of n and $\bar{P}_J$. After finding ϕ_k as a function of k, n and $\bar{P}_J$, then Eq. (19) implies that

$$\left(\frac{B}{f_0}\right)^{(k)} = \frac{2}{\pi} \frac{\phi_k}{d_{\lambda/2}\sin\theta}. \tag{47}$$

For example, to find $(B/f_0)^{(3)}$ when all the conditions of Eqs. (46) hold except (b), we find from Fig. 7 that for $\bar{P}_J = 30$ dB and $n = 10$ that $\phi_3 = 0.1$. Hence using Eq. (47), $(B/f_0)^{(3)} = 0.9$. Thus under these conditions, the bandwidth of the jammer must be 9% of the center frequency for the third largest eigenvalue to be significant.

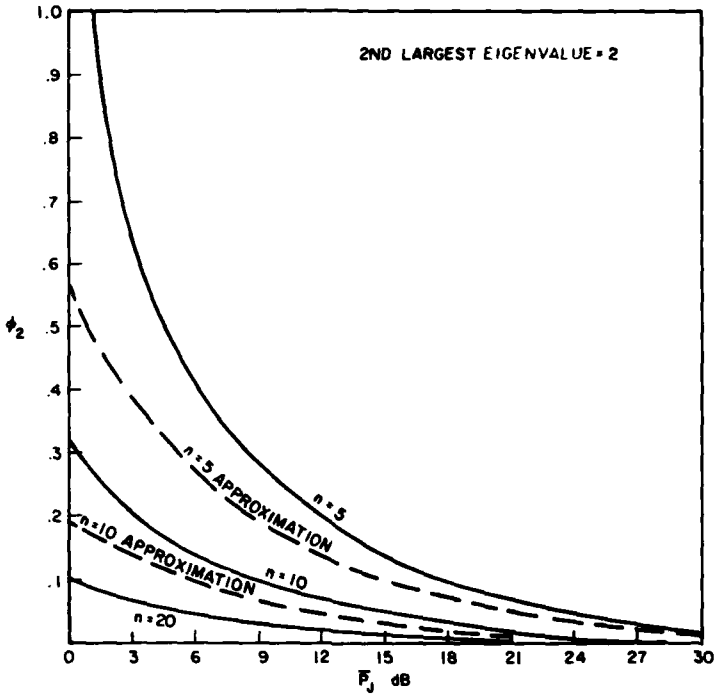

Fig. 6 — ϕ_2 *vs* $\bar{P}_J$ and n, 2nd largest eigenvalue = 2

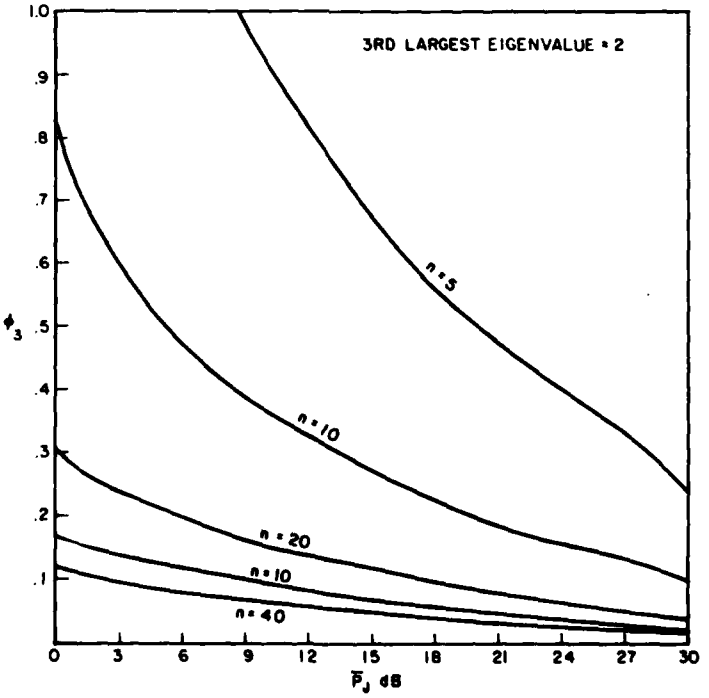

Fig. 7 — ϕ_2 *vs* $\bar{P}_J$ and n, 3rd largest eigenvalue = 2

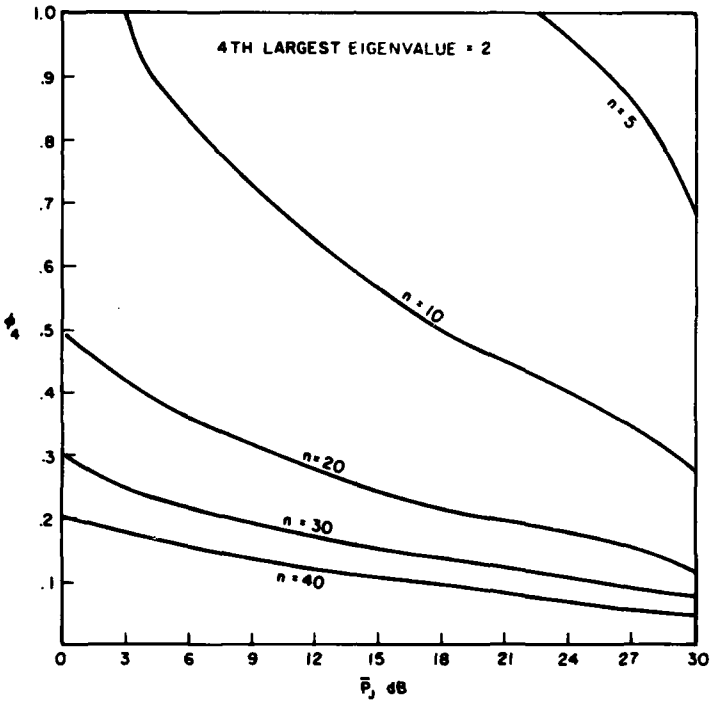

Fig. 8 — ϕ_4 *vs* $\bar{P}_J$ and n, 4th largest eigenvalue = 2

We have also shown in Fig. 6 the approximate value of ϕ_2 as calculated using the approximation given by Eq. (42). Examining Eq. (42), if we set $\hat{\lambda}_{J_2} = 1$, corresponding to the case where the second largest eigenvalue of $\hat{M}$ is two, then

$$\phi_2 = \frac{6}{(\bar{P}_J\, n(n^2-1))^{1/2}}. \tag{48}$$

We see from Fig. 6 that this approximation improves as $\bar{P}_J$ or n increase. This is reasonable because our original analysis assumed that ϕ is small and, hence, for larger $\bar{P}_J$ or n, Eq. (48) implies that ϕ_2 will become smaller.

An important point to be noted from the curves of Figs. 6, 7, and 8 is the quantum nature of ϕ_2, ϕ_3, and ϕ_4 as a function of the kth largest eigenvalue, $k = 2, 3, 4$. If we compare Fig. 6 with Fig. 7, we see that for a given n and $\bar{P}_J$, there is a large difference between ϕ_2 and ϕ_3. This can also be seen in comparing ϕ_3 with ϕ_4 for a given n and $\bar{P}_J$ from the curves of Fig. 7 and 8. This phenomenon is further illustrated in Fig. 9 where we have plotted ϕ *vs* $\bar{P}_J$ for $n = 10$. (Note that $\phi = \phi_2$, ϕ_3, or ϕ_4 for $k = 2$, 3, and 4 respectively.) For example if $n = 10$ and $\bar{P}_J = 9$ dB, then from the curves in Fig. 9, $\phi_2 = 0.1$ and $\phi_3 = 0.39$. Thus, Eq. (47) implies that the jammer bandwidth where the third eigenvalue degrades performance is approximately four times greater than the bandwidth where the second eigenvalue degrades performance. This corresponds to the two jammer bandwidths where two and three degrees of freedom are necessary to null the jammer effectively. Hence, we expect the adaptive array's performance as measured by the output signal-to-noise ratios to degrade in discrete steps as the input noise bandwidth increases.

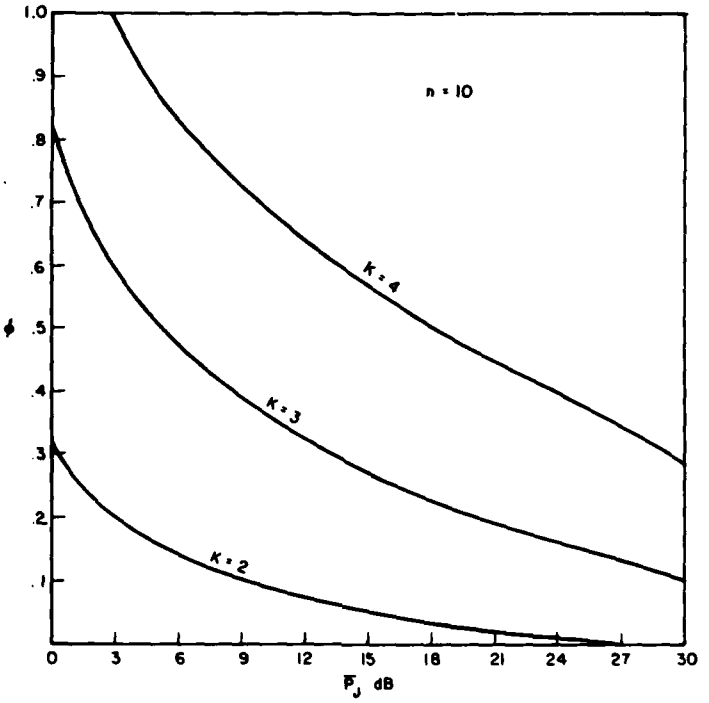

Fig. 9 — ϕ *vs* $\bar{P}_J$ for $k = 2, 3, 4$; $n = 10$

CONCLUSIONS

The relative measures of the eigenvalues of the noise covariance matrix of an adaptive array that is subjected to a non-narrowband jamming source have been investigated. These measures are important because they determine the convergence rate and the upper limit of the output signal-to-noise ratio of the adaptive array. It was found that the adaptive array's performance as measured by the output signal-to-noise ratio degrades in quantum jumps as the input noise-bandwidth increases. A methodology was developed whereby given the number of elements of the array, the array spacing, the array element antenna pattern, the power, and direction of arrival of the external jammer, then these discrete bandwidths of the jammer that limit the output signal-to-noise ratio can be calculated.

REFERENCES

1. S.P. Applebaum, "Adaptive Arrays," *IEEE Trans. on Antennas and Propagation*, **AP-24**, No. 5, 585-598, Sept. 1976; also Syracuse Univ. Res. Corp., Rep. SPL TR 66-1, August 1966.

2. B. Widrow, P.E. Mantey, L.J. Griffiths, and B.B. Goode, "Adaptive Antenna Systems," *Proc. IEEE*, **55**, 2143-2159, Dec. 1967.

3. L. E. Brennan, E.L. Pugh, and I.S. Reed, "Control-Loop Noise in Adaptive Array Antennas," *IEEE Trans. Aerosp. Electron. Syst.*, **AES-7**, 254-262, March 1971.

4. L.E. Brennan and I.S. Reed, "Theory of Adaptive Radar," *IEEE Trans. Aerosp. Electron. Syst.*, **AES-9**, 237-252, March 1973.

5. W.F. Gabriel, "Adaptive Arrays—An Introduction," *Proc. of IEEE*, **64**, 239-272, Feb. 1976.

6. D.J. Chapman, "Partial Adaptivity for the Large Array," *IEEE Trans. on Antennas and Propagation*, **AP-24**, No. 5, 685-696, Sept. 1976.